Optical and electrical properties of graphene oxide and reduced graphene oxide films deposited onto glass and Ecoflex® substrates towards organic solar cells

Agnieszka Iwan[1*], Felipe Caballero-Briones[2], Krzysztof A. Bogdanowicz[1], José D. O. Barceinas-Sánchez[3], Wojciech Przybyl[1], Adam Januszko[1], Javier A. Baron-Miranda[2], Ana P. Espinosa-Ramirez[3], Jesus Guerrero-Contreras[4]**

[1]*Military Institute of Engineer Technology, Obornicka 136 str., Wroclaw 50-961, Poland*
[2]*Instituto Politécnico Nacional, Materials and Technologies for Energy, Health and Environment (GESMAT), CICATA Altamira. Km 14.5 Carretera Tampico-Puerto Industrial Altamira, 89600 Altamira, México*
[3]*Instituto Politécnico Nacional, Laboratorio de Manufactura y Procesamiento de Materiales, CICATA Querétaro, Cerro Blanco 141 Colinas del Cimatario, 76090 Querétaro, México.*
[4]*Centro de Investigación en Química Aplicada, Laboratorio Nacional de Materiales Grafénicos, Blvd. Enrique Reyna No. 140, Col. San José de los Cerritos, 25294 Saltillo, Coah. Mexico*

DOI: 10.5185/amlett.2018.1870
www.vbripress.com/aml

Abstract

Graphene oxide (GO) was synthesized using modified Hummers method. GO films were deposited by doctor blade onto glass slides and Ecoflex® membranes using GO suspensions, or dip-coated onto molecular functionalized glass substrates. Doctor bladed films were studied by optical transmittance, linear sweep voltammetry and by thermal imaging under applied potential. Dip coated films were reduced with different chemical agents to produce transparent, conductive, reduced graphene oxide (rGO) films that were characterized by optical transmittance, current sensing atomic force microscopy and X-ray photoelectron spectroscopy. Doctor bladed GO films were mechanically stable, with resistances ranging 10^6 to 10^{11} Ω depending on the film thickness, which in turn depended on the GO precursor solution concentration. Thermal imaging did not provided evidence of visible voltage-activated conduction. The best reduction treatment to obtain transparent and conductive rGO films, comprised a primary reduction with $NaBH_4$ followed by an air annealing at 120 ºC. Conductive atomic force microscopy indicated that rGO film conductivity is governed by the superposition of individual sheet and X-ray photoelectron spectroscopy suggested that the C/O ratio is not determinant for conduction. The better reduced films had transmittances ca. 85% with sheet resistances around 10^3 Ω/sq, making them feasible as transparent electrodes. Finally, a short discussion about location of GO/rGO in organic solar cells is presented.

Keywords: Graphene oxide, reduced graphene oxide, Ecoflex®, organic solar cells, flexible devices.

Introduction

Recently, graphene or graphene oxide has been tested either as transparent conductive electrodes or as other layers in different devices such as light-emitting diodes, field effect transistors, organic photovoltaic devices, fuel cells or ultracapacitors [**1-3**]. However, perspectives of graphene applications and commercialization require large-scale, good quality, low-cost and eco-friendly production procedures. The main issue concerning solar cells applications is to improve the electrical and mechanical properties of graphene. For example, graphene oxide synthesized by chemical methods in the large-scale production, has to be reduced to increase its conductivity but the achievable conductivity depends on the reduction treatments as well as on the original molecular structure of graphene oxide [**4**], which in turns depends on the repeatability and variations of the synthetic process [**4-8**]. With respect to mechanical properties, the adherence of graphene oxide (GO) and reduced graphene oxide (rGO) films onto polymer and rigid substrates is a critical issue in transparent electrodes; the need of anchoring molecules and the variations of the adherence mechanism (perpendicular or parallel to the substrate) is an issue to be addressed as it affects both the electrical and interfacial properties of the devices.

On the other hand, graphene films as electrodes in flexible organic solar cells have been recently reported [**9**], however, to the best of our knowledge, GO deposition onto the biodegradable substrate Ecoflex® has not been reported towards stable, ecologically-friendly photovoltaics; however, composites of Ecoflex® with carbon nanotubes have been already tested in supercapacitors [**10**] and skin-mountable strain sensors [**11, 12**].

In the present contribution we selected Ecoflex® as flexible substrate for several reasons such as:

- excellent mechanical properties [**11, 13**].
- due to strong interfacial bonding between the carbon nanotubes and the Ecoflex® matrix [**11**], we believe that similar interactions would happen between GO and Ecoflex®.
- Ecoflex® is water and weather resistant, making it suitable for long term applications [**11**].

In the present work, GO has been synthesized via modified Hummers method [**4**]. GO films were deposited by doctor blade onto glass and Ecoflex®/glass substrates and onto molecular-functionalized glass substrates to be further reduced by chemical methods. The effect of deposition conditions as well as the different reduction treatments on the conductivity and optical properties of graphene oxide based electrodes is discussed in term of their applicability to organic solar cells.

Finally, based on literature data and our previous work [**14**] we discuss the effect of graphene oxide on the efficiency of organic solar cells taking into consideration the location of GO in the device.

Experimental

Materials

All chemicals were used as received from Sigma-Aldrich without additional purification. Biodegradable aliphatic-aromatic copolyester (produced by BASF under the commercial mark Ecoflex®) was used as received.

Synthesis of graphene oxide (GO)

The GO synthesis procedure of our group has been described in ref. [**4**]. Briefly, synthetic graphite, H_2SO_4, $KMnO_4$ and $NaNO_3$ were mixed, let react during 120 min at 5º C, 30 min at 35º C and 30 min at 98º C to finish the reaction by adding H_2O_2/water. The product was washed with HCl 5% and DI water, and let dry overnight at 60º C. Powder was molten with an agate mortar and aqueous solutions were prepared from it by sonicating proper amounts of powder during 1 h. Soda-lime glass slides were cut into 2.5 x 2.5 cm^2 pieces, thoroughly washed with neutral liquid detergent, rinsed with deionized water, soaked into piranha solution (H_2SO_4:H_2O_2 1:1), rinsed with deionized water, dried in a N_2 stream and kept at 70º C

GO films preparation on glass support

GO films on soda-lime glass substrates were prepared using GO solutions with 0.1 mg/mL, 5 mg/mL, 10 mg/mL and 40 mg/mL concentrations respectively. The solution was spread on a glass plates with a casting knife with a 100 µm gap and was left overnight to dry on air.

GO films preparation on flexible support

An Ecoflex® solution in methylene chloride (20% w/v) was casted over glass surface using a casting knife with 200 µm gap and was left to evaporate. Next, GO aqueous suspension with different concentrations prepared as described above, were spread using casting knife with a 100 µm gap and was left overnight to dry on air.

GO films

A freshly prepared 3% v/v solution of 3-aminopropyl trietoxysilane (APTES) in toluene was prepared and the clean substrates were introduced during 1 h, with the APTES solution at 70º C. Functionalized substrates were rinsed successively in toluene, ethanol and water and dried in N_2 stream. GO was deposited by immersing the APTES/glass substrates in an aqueous GO solution 0.05 mg/mg during 1 h at 70º C, to be finally rinsed with DI water, dry in N_2 stream and kept in the oven until reduction. Ecoflex® functionalization was not achievable because damage by solubility in toluene. Future work is intended to test APTES or another functionalization using compatible solvents. Several samples of each method were prepared for a preliminary variability assessment of the reduction methods.

rGO/glass films

Graphene oxide films were reduced by 5 different methods to latter study the electrical and optical behavior.

Method 1:
Films were introduced into a sealed chamber and exposed to hydrazine vapor at 70º C during 18 h, afterwards the films were rinsed with water and let dry in the oven at 70º C. Films changed from brown to black. A second reduction process was done by introducing the films into 0.1 M $NaBH_4$ solution by 2 h at room temperature. Films were rinsed, dried and kept into a desiccator until characterization.

Method 2:
The first reduction step was done with hydrazine as before and the second reduction using a 0.1 M sodium citrate solution at pH 10 for 2 h at 70º C.

Method 3:
First reduction was done by immersing the film in a 0.1 M $NaBH_4$ solution during 2 h at room temperature. The second reduction was a thermal treatment at 120º C in air during 2 h.

Method 4:
The first reduction step was done with hydrazine as in Method 1 and 2, and the second reduction was done in a D-glucose solution at pH 10, during 2 h at 70º C.

Method 5:
The first reduction step was done with hydrazine as in Method 1 and 2, and the second reduction was done by introducing the substrate into a Zn/HCl aqueous solution (1 g Zn, 5% HCl) during 2 h before rinsing and drying.

Method 6:
Same as method 5, although in this case, Zn powder was directly spread onto the film and pure HCl was dropped onto Zn powder. The method largely damaged the film, thus it was not further considered.

An additional GO film named X was prepared with the GO suspension at 5 mg/mL and only a single hydrazine reduction step was used.

Characterizations

Detailed characterization of our GO powders has been described elsewhere [**4, 14**]. Briefly, X-ray diffraction, infrared spectroscopy and transmission electron microscopy were used to study degree of exfoliation, molecular structure and sheet morphology.

The thickness, electrical conductivity and transmittance was studied in the doctor blade deposited films. The thicknesses was measured using Baker Electronic Outside Micrometre IP54, measurement range 0-25 mm and measurement error 0.001 mm. Linear sweep voltammetry (LSV) measurements were performed using Autolab PGstat M204 in potentiostatic mode with current ranging from 10 nA to 100 mA, potential range from 0 V to 4.9 V, step 0.00244 V and scan rate 0.02 Vs^{-1}. The experimental setup included two brass electrodes on adjustable clamps separated in a distance of 1 cm. In order to improve the contact between the electrodes and samples an electroconductive CircuitWorks® Silver Conductive Grease (volume resistivity < 0.01 Ω-cm) was used. For the measurements samples have a minimum size of 1.5 cm × 1.5 cm. Thermal behavior was observed using thermografic camera (VIGOcam v50, VIGO System S.A, Poland) while applying voltage bias between 0 and 32 V using a DC conventional source. UV-Vis experiments were performed in transmittance mode using UV-Visible-Near Infrared JascoV-770 spectrophotometer (Germany) equipped with ILN-925 integrating sphere accessory for solid samples. The measured range 200-1100 nm with scan rate 100 nm/min with correction on dark baseline. The spectra in the case of Ecoflex®-supported samples were performed on a samples fixed to a glass slide by edges outside the measurement window, ensuring flat surface during measurement.

The electrical and optical properties as well as the composition of dip-coated films (either GO and rGO) was studied. Film resistivity of the rGO films was measured in the Van der Paw setup without using electrical contacts. The system consisted in a home-made 4-point, a power source, a multimeter and two high impedance (1 Tohm) electrometers, all by Keithley. Local electrical measurements of the rGO films deposited onto glass substrates were done by current sensing atomic force microscopy (CAFM) using a TT AFM Workshop microscope and Pt coating Cr-Si tips with force constant of 40 N/m, directly applying the bias voltage between the tip and the rGO film in contact mode. Transmittance spectra of the rGO/glass films were acquired in a Perkin Elmer Lambda 40 spectrometer in the 200-1100 range. X-ray photoelectron spectroscopy was measured in a Thermo Scientific K alpha XPS instrument using monochromatic Al K α X-rays and low energy electron flooding to avoid charging. Spectra were acquired without Ar erosion and survey spectra of all the samples (resolution of 1 eV) as well as high resolution spectra (0.2 eV) around the C 1s and O 1s peaks were made.

Results and discussion

GO analyses

GO characterization produced by our experimental setup has been thoroughly described before [**4,14**], however for the sake of clarity, **(Fig. 1A)** presents transmission electron images showing the layered nature of the product; **(Fig. 1B)** are the X-ray diffractograms of graphite and GO where the characteristic peaks of GO and graphite are clearly indicated; **(Fig. 1C)** shows the infrared spectrum of GO featuring carboxyl, phenolic, ether and epoxy related bands; finally, **(Fig. 1D)** shows the XPS survey spectra of graphite and GO where the C 1s and O 1s are observed, and the calculated C/O ratio for GO powder is ca. 4.5. Previous results have shown that GO powder resistance is 24 KOhm compared with ca. 2.5 KOhm for pristine graphite [**14**].

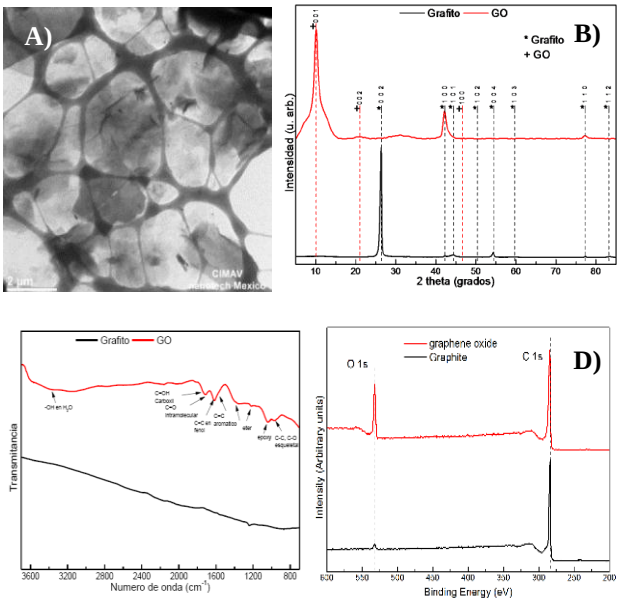

Fig.1. GO and graphite characterizations: A) TEM image (scale bar is 2 μm) of GO powder; B) XRD; C) FTIR spectra; D) XPS spectra.

GO films, adherence and mechanical stability

After casting all solutions on glass substrate, uniform layers were obtained as it can be seen in the **Fig. 2A**. Only for the case of 0.1 mg/mL concentration some small agglomerates of GO particles were distinguishable, possibly because the non-wettability of the glass substrate. Also in the case of Ecoflex® support **(Fig 2B)** uniform layers were obtained without any visible prove for agglomeration. All layers seem uniformly colored and the thickness of GO layers seems equal for all

concentration (4 µm) within the experimental error. Only the film prepared with the GO solution at 40 mg/mL got broken while pilled off in the glass support used to cast Ecoflex® film. All the films were fully flexible.

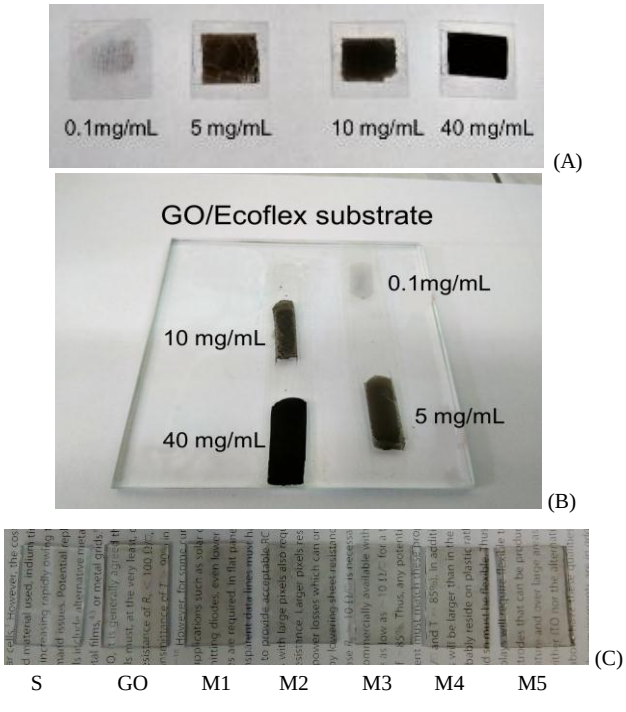

Fig. 2. Photographs of the prepared films: A) doctor bladed GO/glass B) Ecoflex® support and C) dip coated rGO/APTES/Glass; the concentration of the precursor GO solutions is indicated. S accounts for glass substrate, GO for unreduced film and M1-M5 for the reduction method.

Fig. 2C display the films dip coated onto APTES functionalized glass, including the glass substrate, the GO film and the rGO films prepared with the methods 1-5. RGO film prepared with the method 6 is not shown because it was partially destroyed during the treatment. In the case of dip coated films the thickness was not measured because resolution limit of the micrometer apparatus, however deposition times were the same, thus similar thicknesses are expected. Films are transparent as readily observed and the color suggests different degree of reduction [**15**].

Optical properties

Fig. 3 represents the transmittance (%T) spectra for GO solutions **(Fig 3A)**; the different GO samples on a glass support **(Fig 3B)** and Ecoflex® **(Fig. 3C)** respectively. The measured GO solutions are shown in the photo inset: a) 0.05 mg/mL prepared from our GO and b) 0.05 mg/mL prepared from a commercial GO (Graphene Supermarket, 5 mg/mL ink). In **Fig. 3A** the transmittance spectra of the 0.05 mg/mL solutions display two absorption peaks at 260 nm and 310 nm, corresponding to the well-known transitions π to π* and n to π* levels already observed in our GO [**4**]. The main difference is the higher extent of the absorption and higher transmittance above the absorption peaks in the commercial solution, possibly due to a better exfoliation degree of the later.

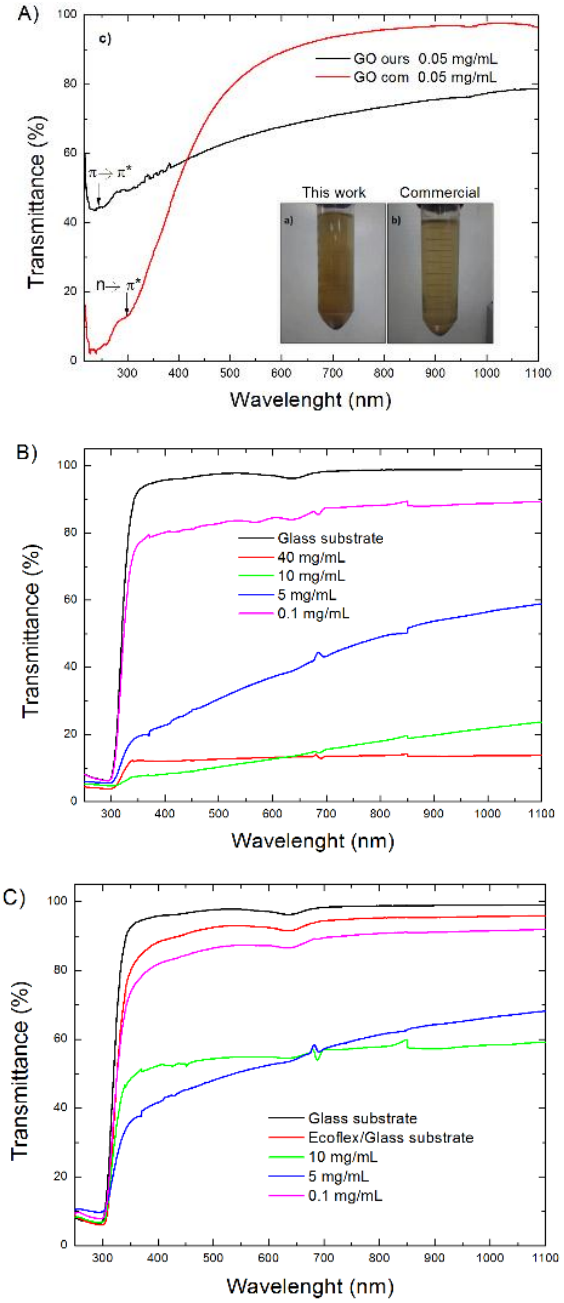

Fig. 3. A) Photographs (a,b) and transmittance spectra c) for GO solutions with 0.05 mg/mL, where a) our GO; b) commercial GO; transmittance spectra of the GO films casted by doctor blade onto B) glass and C) Ecoflex®/glass substrates.

In **Fig. 3B** the spectra show an increasing transmittance upon reduction of the concentration of the GO solution; the transmittance in the visible range increases from around 15% to 80%, a range suitable for transparent electrodes, consistently with the photographs in **Fig. 2a**. The characteristic absorption peaks at 230 and 310 nm were not observed below the glass absorption edge. In the case of GO layers on Ecoflex® support **(Fig. 3C)** a similar tendency is observed, although

10-15% higher mean transmittance compared with GO in glass substrate is observed, which could be attributed to a more uniform layer formation because the Ecoflex® support is more wettable than glass. Both series present a small transmittance below the glass absorption edge at ca. 300 nm, indicating the presence of pinholes or non-uniform deposition.

Film performance as transparent electrode

The preparation of electrically conductive samples was achieved for almost all GO layers supported both on glass and Ecoflex® supports with electrical resistance between 10^8-10^{11} Ω, as calculated from linear sweep voltammetry. Also, the GO and rGO films prepared onto APTES substrates displayed sheet resistances (Rs) between 10^3-10^6 Ω, as calculated from Van der Paw measurements. The influence of the deposition parameters and the reduction methods on the electrical and optical properties is summarized in **Fig. 4.** Also, the figure of merit for transparent electrodes, T^{10}@550nm/Rs [**16**] for the prepared films, and the C/O ratio for selected rGO samples, is presented in **Fig. 4(A, B)**.

Fig. 4A presents the transmittance at 550 nm and the electrical resistance of the GO films prepared by doctor-blade casting onto glass substrates. It can be observed that film transmittance reduces proportionally to the increase in the precursor GO solution (from 0.1 mg/mL to 40 mg/mL). On the other hand, the film resistance reaches a minimum value in the film prepared with the 5 mg/mL GO solution. Lower solution concentration together with particle agglomeration lead to higher resistance, while film compaction with increasing GO solution concentration allow resistance reduction. The large Rs values could be explained because GO was not reduced, but also by trapped water within the film as evident by the observed agglomerates (see discussion of Fig. 2a) and pinholes caused by low wettability and water evaporation (see discussion of Fig. 3A). **Fig 4A** inset displays the Haacke Figure of Merit (FoM) [**16**] for the GO films prepared onto glass and Ecoflex® substrates. In both series of samples the better FoM is obtained for the films prepared with the 5 mg/mL GO solution, although a more reduced performance is observed for the GO films onto Ecoflex®, because these films displayed film resistances in the order or 10^{11} Ω. The reason behind the large resistance of GO/Ecoflex® substrates is not well understood at the present time. As the reduced performance of the films is mostly attributed to the film defects caused by the deposition procedure, the performance of the dip-coated GO and rGO films deposited onto APTES modified substrates is revised on **Fig. 4B.**

Fig. 4B displays the transmittance at 550 nm and the sheet resistance as well as the FoM of 17 films deposited onto APTES/glass substrates from a 0.05 mg/mL GO precursor solution: a GO film, 16 rGO films reduced with the 6 methods described above and an additional film named X, prepared with a 5 mg/mL GO solution, corresponding to the best doctor bladed film prepared onto glass substrate, with only a single hydrazine reduction step. **Fig. 4B** also presents the C/O ratio of selected samples measured by XPS.

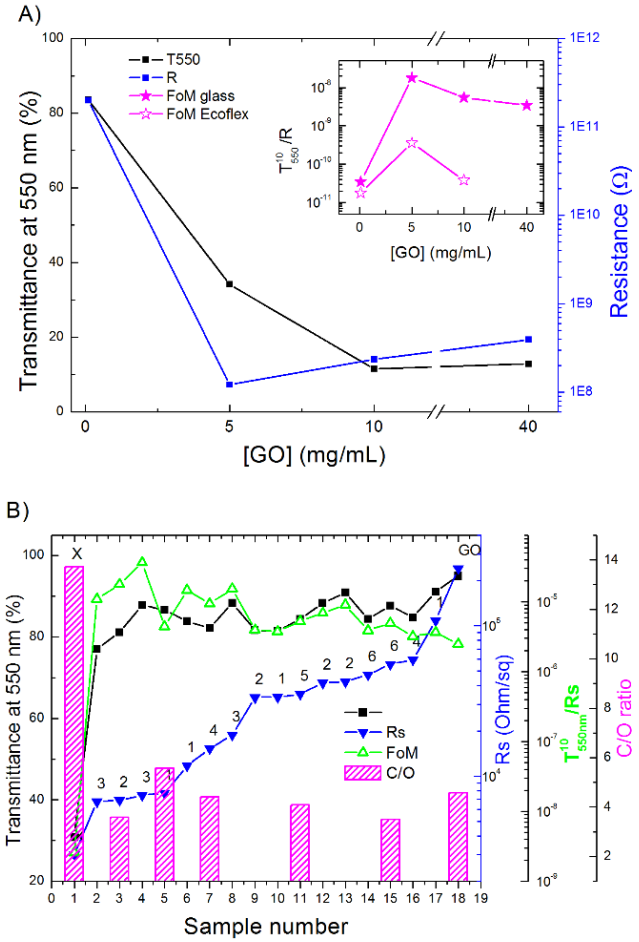

Fig. 4. Transmittance at 550 nm and resistance of the GO films A) deposited by doctor blade onto glass substrates vs the GO solution concentration; inset: Haacke FoM for GO films onto glass and Ecoflex®. B) For the 18 films prepared onto APTES/glass substrates and reduced with the Methods 1-6; Haacke FoM and C/O ratio from XPS are also displayed as additional y-axis.

Films are organized with respect to increasing sheet resistance in the range of 10^3-10^6 Ω/sq. First noticeable observation is the dispersion of film resistance values within the reduction methods, although some tendencies can be inferred; *i.e.* films reduced with the method 3 (2/3 of the measured films) tends to be less resistive (< $1x10^4$ Ω/sq) than those reduced with method 2 (*ca.* $5x10^5$ Ω/sq; 3/4 of the measured values), and method 6 leads to the higher Rs values. The absolute maximum in the Haacke FoM is obtained with method 3, *i.e.* a first reduction with $NaBH_4$ followed with thermal treatment at 120º C. Sample X, prepared with a GO concentration 5 mg/mL, is notoriously conductive (3 kΩ/sq) but is very opaque (30 %T@550 nm) in the order of that prepared by doctor blade. Consequently, the FoM of film X is the lowest. In the case of GO film, it has the higher transparency (*ca.* 95%@550 nm), and the highest Rs (*ca.* 240 kΩ/sq) and a FoM one magnitude less than the best one. The variations

of film transmittance can be related on one hand, with the reduction ratio [**15**] and on the other hand, with the number of graphene sheet [**17**]; considering that a single graphene sheet reduces transmittance by 2.3%, an estimate of 3-8 graphene sheet was deposited. With respect to the C/O ratio, there is a slight correlation with the film resistance, but due to the dispersion within the reduction methods, there is a need of strength the control over the reduction conditions. Raman spectra (not shown) also suggest a correlation of the I_D/I_G ratio with the reduction rate [**18**] within the dispersion found in the experimental results. An interesting observation is that the C/O ratio is below of that of GO in samples 3, 7, 11 and 15. The high resolution XPS spectra (not shown) did display subtle differences between the methods; after deconvolution, C1s spectra show defined C=C (sp^2) and C=O/O-C-O (phenol, epoxy), C(O)OH (sp^3) related peaks at 284.8 and 288.2 eV respectively [19,20]; in the O 1s spectra, peaks at 531.5 eV, 532 eV, 533.3 eV, 534.7 eV, 535.8 eV, and 538.5 eV, related to multiple rings, carboxylic, phenyl, ketone, ether and hydroxyl moieties are observed [**21**]. GO films does not display the 538.5 eV peak related with ketone/anhydride groups and it is present after reduction. GO reduction mechanisms are poorly understood, mostly because the complex nature of the GO molecular structure itself, on which there is not universal consensus and its highly dependent on the preparation method and carbon source. For example, GO powders prepared with our method features carboxyl, phenolic, ether and epoxy moieties. $NaBH_4$ reduces carboxylic, ketone and aldehyde moieties to hydroxyl [**19**], whereas N_2H_4 reduce epoxide and hydroxyl although large proportion of carboxyl and hydroxyl could remain in the reduced product, which in turn would explains the apparent decrease of C/O ratio in samples 3, 7, 11 and 15 with respect to GO. Complete thermal reduction would occur above 1000º C, but it is reported a large mass loss below 200º C [**20**], justifying the results obtained with the Method 3.

Thermal images of GO films

Thermal images of the GO thin films with various amounts of GO on glass and Ecoflex® substrate were acquired with a thermographic camera at different bias substrates, to observe IR emission due to current flux, i.e. Joule heating and detect possible current shunts. **Fig. 5a, b)** presents the thermal images obtained on the films prepared onto glass substrate with increasing GO solution concentration (5, 10 and 40 mg/mL) tested at 0 V and 32 V respectively **(Fig. 5a).** The first observation is an increase in the mean temperature at the higher potential from *ca.* 22.5º C to *ca.* 26º C, consistently with the higher current flux thru the film. The presence of colder regions in the films prepared with 10 mg/mL and 40 mg/mL GO solutions suggest current shunts, which could be related with the pinholes or defects that cause the resistance increase in these films (see discussion above). **Fig 5b)** displays the thermal images of the film prepared with the GO solution of 5 mg/mL, which has the lower resistance, at increasing bias voltages. From about 20 V the mean temperature is similar in the images (*ca.* 26º C) and also the temperature within the entire image including the metal contact is homogeneous, suggesting a voltage activated conductivity, an interesting property recently applied in graphene-based LEDs [**22**]. **Fig. 5c)** compares the images obtained in the films prepared onto glass and Ecoflex® with the 10 mg/mL GO solution at 0 and 28 V. The film prepared onto Ecoflex® display a more homogeneous IR emission distribution, in accordance with its better homogeneity, but lower temperature in accordance to its higher electrical resistance.

Nanoelectrical characterization of rGO films

The local electrical behavior of the reduced GO films was studied by CAFM in order to investigate the mechanisms of conduction. **Fig. 6** presents the nanoelectrical characterization of the rGO films reduced with methods 1-4 as well as an indium tin oxide (ITO) film measured for comparison. The topographical and electrical images as well as the height and current distributions are presented. Films prepared by method 5 lose adherence and AFM imaging was not possible.

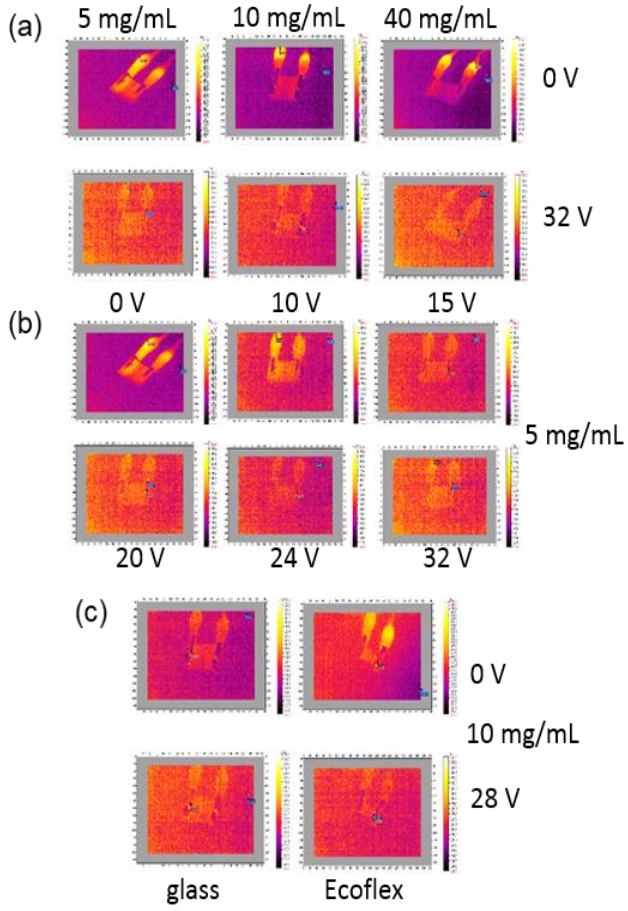

Fig. 5. IR images from thermal camera of: (a) GO/glass (5, 10, 40 mg/mL) at 0 V and 32 V; (b) GO/glass (5 mg/mL) at 0 V, 10 V, 15 V, 20 V, 24 V and 32 V; (c) GO/glass and GO/Ecoflex® (10 mg/mL) at 10 V and 28 V. The thermal scale for all images ranged from 22.0 ºC to 28.5 C. Brighter feature is metal clip used as contact.

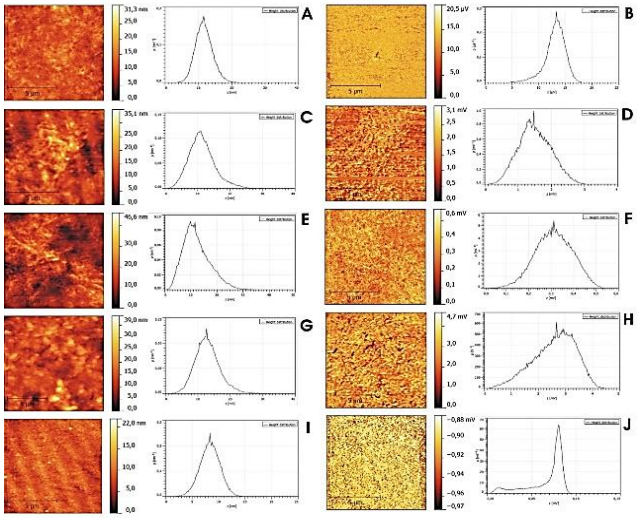

Fig 6. 10 x 10 μm^2 CAFM images of the rGO films and ITO substrate with 100 Ohm/sq (A-B is sample prepared with method 1; C-D sample prepared with method 2; E-F sample prepared with method 3; G-H sample prepared with method 4 and I-J, ITO). Left images and histograms are topographic map and height distributions; right images and histograms are electrical maps and current distributions respectively.

The comparison between the topographic and current images indicate a correlation between film uniformity and current flux. The dark regions in the topographic map coincide with the dark regions in the current images and also the height distribution is closely related with the current distribution as seen in the histograms. The narrowest current distribution is achieved in the film prepared with Method 1 with the narrowest height distribution **(Fig 6 A-B)**. **Table 1** presents the calculated R_{rms} and the current ranges obtained from the images A-J. The variations in film roughness are directly related with the current fluxes (Methods 2-4) and (Method 3-ITO), confirming the role of the sheet boundaries in the electrical conductivity. It is noteworthy that rGO roughness values are close to that of ITO, making our rGO films suitable as electrodes in organic solar cells.

Table 1. Roughness and current distribution ranges of the rGO films prepared with different methods.

Method	R_{rms} (nm)	Current range (nA)
1	2.65	0.022–0.030
2	4.20	2–4
3	5.30	0.2–0.4
4	4.15	4–7
5	6.7	NA
ITO	2	0.14–0.18

GO in organic photovoltaics: Review

Ambient, mechanical, and long term stability of organic solar cells (OSCs) together with their flexibility are capital issues at the present time for technology scaling. Each layer in organic solar cell suffers from not ideal morphology, interface behavior or chemical instability [**23-25**]. Among the proposed solutions for these problems large attention has been paid to graphene and GO [**3**]. Graphene/GO can be applied as a replacement for ITO (anode) or/and Al (cathode) for the transparent electrode of polymer solar cells as depicted in **Fig. 7** [**3,9, 26-30**]. Also, both organic layers in solar cells, active and hole transporting layers can be doped with GO to improve efficiency of the devices [**3**].

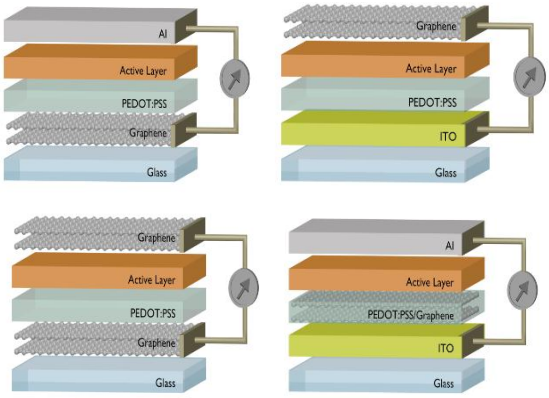

Fig. 7. Organic solar cells with GO in hole transporting layer, anode, cathode and both electrodes.

For example, in our previous work [14] we investigated the influence of (i) concentration of GO in HTL, (ii) type of polymer used in active layer (poly(3-hexylthiophene) - P3HT or poly({4,8-bis[(2-ethylhexyl)oxy]benzo[1,2-b:4,5-b′]dithiophene-2,6-diyl}{3-fluoro-2-[(2-ethylhexyl) carbonyl]thieno[3,4-b]thiophenediyl}) - PTB7, (iii) annealing temperature of the active layer and (iv) place where GO is incorporated in the devices. The best performance (PCE = 5.22 %) was obtained for a device with the ITO/(PEDOT:PSS):GO (1:1)/PTB7:$PC_{71}BM$/Al architecture (PEDOT:PSS: poly (3,4-ethylenedioxythiophene) : poly (styrenesulfonic acid, $PC_{71}BM$: [6,6]-phenyl C71 butyric acid methyl ester), and better photovoltaic parameters were obtained for P3HT:PCBM active layer annealed at 130º C (PCBM: [6,6]-phenyl-C61-butyric acid methyl ester) [**14**]. With respect to the use of graphene in semi-transparent electrodes, either in the anode, the cathode or both electrodes to allow bifacial cell illumination, there is a report for an inverted OSC with the architecture ITO/ZnO/P3HT: PCBM/GO/graphene with 8 graphene layers; herewith a PCE_{max} = 2.04 % was reported when illuminating from graphene side, and 2.40 % illuminating from ITO side [29]. In bifacial illumination, the highest reported value of PCE was achieved by Liu *et al.* [**30**] for a ITO/ZnO/PTB7: PCBM/PEDOT: PSS/graphene device, *i.e.* PCE = 4.20 % and 3.75 % illuminating from graphene and from ITO side, respectively. On the other hand, perovskite solar cells with graphene as electrode were widely investigated by Yoon *et al.* [**9**]. A device with improved mechanical stability (PEN/graphene/MoO_3/ PEDOT: PSS/$MAPbI_3$/C_{60}/BCP/LiF/Al, where PEN: poly (ethylene naphthalate), BCP: bathocuproine, $MAPbI_3$: $CH_3NH_3PbI_3$) exhibited comparable efficiency with the device with ITO (PCE = 16.8 % and 17.3 %, respectively).

Conclusions

In this work graphene oxide and reduced graphene oxide films were prepared onto glass and onto a flexible substrate (Ecoflex®) using different deposition approaches. First, the optical and electrical properties of films casted from solutions with increasing GO concentration was analyzed. Films prepared onto glass are less uniform but higher transparent electrode Haacke's figure of merit values were obtained. Voltage activated conductivity was inferred from thermal images. Film resistance reaches a minimum with the solution prepared with 5 mg/mL GO. Secondly, the optical and electrical behavior of GO films deposited onto APTES functionalized substrates followed by chemical reduction with different procedures was studied, to assess the feasibility of rGO applications in transparent electrodes in OSCs. Films were more adherent and uniform than the casted ones. Sheet resistances as low as 10^3 Ω/sq and transmittances above 80% were achieved. Although some dispersion between the results, the best reduction procedure seems to be a first $NaBH_4$ step, followed by a mild thermal reduction. The conduction mechanism studied by conductive atomic force microscopy seems to be related with the individual sheet piling. Finally, a discussion on GO and rGO applications in OSCs was done. Attending our previous and present results as well as the discussed literature, the following goals are devised:

1. Perform a statistically significant assessment of the GO reduction methods, with emphasis in the greener ones.
2. Construct OSCs using with our best rGO/glass films as front, back or both electrodes, including the use of GO in the HTL as reported previously.
3. Introduce Ecoflex® as a flexible, green substrate to build OSCs, after essays of chemical stability towards functionalization, GO deposition and reduction.

Acknowledgements

FCB acknowledges SIP-IPN project 20161804, and SNI, EDI and SIBE grants for financial support. Authors thank F.J. Espinosa-Magaña (NANOLAB-CIMAV), P. Quintana-Owen and W. Cauich at LANNBIO-Merida (CONACYT Grants FOMIX-Yucatan 2008-108160 and LAB-2009-01 123913) for TEM and XPS characterization respectively as well as to B. Boharewicz and I. Tazbir at IEL Wroclaw for solar cell fabrication.

Author's contributions

Authors declare no competing financial or other conflict of interest.

References

1. Sahoo N.G.; Pan, Y.; Li, L.; Chan, S.H.; *Adv. Mater.*, **2012**, *24*, 4203. **DOI:** 10.1002/adma.201104971
2. Wu, Z-S.; Zhou, G.; Yin, L-C.; Ren, W.; Li, F.; Cheng H-M.; *Nano Energy*, **2012**, *1*, 107. **DOI:** 10.1016/j.nanoen.2011.11.001
3. Iwan, A.; Chuchmala, A.; *Prog. Polym. Sci.*. **2012**, *37*, 1805. **DOI:** 10.1016/j.progpolymsci.2012.08.001
4. Guerrero-Contreras, J.; Caballero-Briones, F.; *Mat. Chem. Phys.*, **2015**, *153*, 209. **DOI:** 10.1016/j.matchemphys.2015.01.005
5. Thakur, A.; Kumar, S.; Sharma, M.; Rangra, V. S.; *Adv. Mater. Lett.* **2016**, *7*, 1029. **DOI:** 10.5185/amlett.2016.6810
6. Dommisa, D. B.; Dash, R. K.; *Adv. Mater. Lett.* **2017**, *8*, 315. **DOI:** 10.5185/amlett.2017.1486
7. Mohan, V. B.; Liu, D.; Jayaraman, K.; Stamm, M.; Bhattacharyya, D.; *Adv. Mater. Lett.* **2016**, *7*, 421. **DOI:** 10.5185/amlett.2016.6123
8. Chamoli, P.; Das, M.K.; Kar, K.K.; *Adv. Mater. Lett.* **2017**, *8*, 217. **DOI:** 10.5185/amlett.2017.6559
9. Yoon, J.; Sung, H.; Lee, G.; Cho, W.; Ahn, N.; Hyun Suk Jung, H. S.; Choi, M.; *Energy Environ. Sci.*, **2017**, *10*, 337. **DOI:** 10.1039/c6ee02650h
10. Chee, W. K.; Lim, H. N.; Zainal, Z.; Huang, N. M.; Harrison, I.; Andou, Y.; *J. Phys. Chem. C*, **2016**, *120*, 4153. **DOI:** 10.1021/acs.jpcc.5b10187
11. Amjadi, M.; Yoon, Y.J.; Park I.; *Nanotechnology*, **2015**, *26*, 375501. **DOI:** 10.1088/0957-4484/26/37/375501
12. Lee, J. W.; Xu, R.; Lee, S.; Jang, K-I.; Yang, Y.; Banks, A.; Yu, K. J.; Kim, J.; Xu, S.; Ma, S.; Jang, S. W.; Won, P.; Li, Y.; Kim, B. H.; Choe, J. Y.; Huh, S.; Kwon, Y. H.; Huang, Y.; Paik, U.; Rogers, J. A.; *PNAS*, **2016**, *113*, 6131. **DOI:** 10.1073/pnas.1605720113
13. Tsui H. Polyesters III - applications and commercial products. In: Doi Y, Steinbuchel A, editors. Polylactides in biopolymers, vol. 4. Weinheim: Wiley-VCH; 2002. p. 1-398.
14. Iwan, A.; Caballero-Briones, F.; Filapek, M.; Boharewicz, B.; Tazbir, I.; Hreniak, A.; Guerrero-Contreras, J.; Solar Energy, **2017**, *146*, 230. **DOI:** 10.1016/j.solener.2017.02.032
15. Becerril H.A., Mao J., Liu Z., Stoltenberg R. M., Bao Z., Chen Y., ACS Nano, **2008**, *2*, 463. **DOI:** 10.1021/nn700375n
16. Haacke, G.; *J. Appl. Phys.*, **1976**, *47*, 4086. **DOI**: 10.1063/1.323240
17. Nair. R.R., R.R.; Blake, P; Grigorenko, A.N.; Novoselov, K.S.; Booth, T.J.; Staube, T.; Peres, N.M.R.; Geim, A. K., *Science*, **2008**, *320*, 1308. **DOI:** 10.1126/science.1156965
18. Pei S., Cheng H.-M.; Carbon, **2012**, *50*, 3210. **DOI:** 10.1016/j.carbon.2011.11.010
19. Dave, K.; Park, K.H.; Dhayal, M.; *RSC Adv.*; **2015**, *5*, 95657. **DOI:** 10.4039/c5ra18880f
20. Chang, H.; Sun, Z.; Saito, M.; Yuan, Q.; Zhang, H.; Li, J.; Wang, Z.; Fujita, T.; Ding, F.; Zheng, Z.; Yan, F.; Wu, H..; Chen, M.; Ikuhara, Y.; *ACS Nano* **2013**, *7*, 6310. **DOI:** 10.1021/nn4023679
21. NIST X-ray Photoelectron Spectroscopy Database 20, Version 4.1 Data compiled and evaluated by Alexander V. Naumkin, Anna Kraut-Vass, Stephen W. Gaarenstroom and Cedric J. Powell, **2012**, U.S. Secretary of Commerce
22. Wang, X.; Tian, H.; Mohammad, M.A.; Li, C. Wu, Yang, Y.; Ren, T-L.; Nat. Comm., 2015, 6, 7767 **DOI:** 10.1038/ncomms8767
23. Zhan, X.; Zhu, D.; *Polym. Chem.* **2010**, *1*, 409. **DOI:** 10.1039/B9PY00325H
24. Li, Y.; *Acc. Chem. Res.*, **2012**, *45*, 723. **DOI:** 10.1021/ar2002446
25. Cai, W.; Gong, X.; Cao, Y.; *Sol. Energ. Mat. Sol. Cells*, **2010**, *94*, 114. **DOI:** 10.1016/j.solmat.2009.10.005
26. Sahoo, N.G.; Pan, Y.; Li L.; Chan S.H.; *Adv. Mater.***2012**,*24*, 4203. **DOI:** http://doi:10.1002/adma.201104971
27. Pan, Z.; Gu, H.; Wu, M-T.; Li, Y.; Chen, Y.; *Opt. Mat. Exp.* **2012**, *2*, 814. **DOI:** 10.1364/OME.2.000814
28. Wan, X.; Huang, Y.; Chen, Y.; *Acc. Chem. Res.* **2012**, *45*, 598. **DOI:** 10.1021/ar200229q
29. Lee, Y.Y.; Tu, K.H.; Yu, C.C.; Li, S.S.; Hwang, J.Y.; Lin, C.C.; Chen, K.H.; Chen, L.C.; Chen, H.L.; Chen, C.W.; *ACS Nano*, **2011**, *5*, 6564. **DOI:** 10.1021/nn201940j
30. Liu, A.; You, P.; Liu, S.; Yan, F.; *ACS Nano*, **2015**, *9*, 12026. **DOI:** 10.1021/acsnano.5b04858

